Dual Character of the Electronic Structure of $YBa_2Cu_4O_8$: The Conduction Bands of CuO_2 Planes and CuO Chains

T. Kondo,[1] R. Khasanov,[2] J. Karpinski,[3] S. M. Kazakov,[3] N. D. Zhigadlo,[3] T. Ohta,[4] H. M. Fretwell,[1] A. D. Palczewski,[1] J. D. Koll,[1] J. Mesot,[5] E. Rotenberg,[4] H. Keller,[2] and A. Kaminski[1]

[1]*Ames Laboratory and Department of Physics and Astronomy, Iowa State University, Ames, Iowa 50011, USA*
[2]*Physik-Institut der Universität Zürich, Winterthurerstrasse 190, CH-8057 Zürich, Switzerland*
[3]*Laboratory for Solid State Physics ETH Zürich, CH-8093 Zürich, Switzerland*
[4]*Advanced Light Source, Berkeley National Laboratory, Berkeley, California 94720, USA*
[5]*Laboratory for Neutron Scattering, ETH Zürich and Paul Scherrer Institute, 5232 Villingen PSI, Switzerland*

(Received 28 August 2006; published 11 April 2007)

We use microprobe angle-resolved photoemission spectroscopy (μARPES) to separately investigate the electronic properties of CuO_2 planes and CuO chains in the high temperature superconductor, $YBa_2Cu_4O_8$. For the CuO_2 planes, a two-dimensional (2D) electronic structure is observed and, in contrast to $Bi_2Sr_2CaCu_2O_{8+\delta}$, the bilayer splitting is almost isotropic and 50% larger, which strongly suggests that bilayer splitting has no direct effect on the superconducting properties. In addition, the scattering rate for the bonding band is about 1.5 times stronger than the antibonding band and is independent of momentum. For the CuO chains, the electronic structure is quasi-one-dimensional and consists of a conduction and insulating band. Finally, we find that the conduction electrons are well confined within the planes and chains with a nontrivial hybridization.

DOI: 10.1103/PhysRevLett.98.157002 PACS numbers: 74.25.Jb, 74.72.Hs, 79.60.−i

Y-Ba-Cu-O (YBCO) is one of the most extensively studied high temperature superconductors due to its early discovery, the availability of high quality single crystals, and excellent technological prospects. The system is particularly interesting from a physical point of view as it combines 2D CuO_2 planes and 1D CuO chains in a single unit cell. Despite this interest, the electronic structure of YBCO has rarely been studied experimentally [1–4], with only one recent Letter [5]. While these studies reveal interesting features, such as an extended van Hove singularity around $(\pi, 0)$ [1] and bilayer band splitting in the nodal direction [5], the handful of published studies should be contrasted with the dozens of detailed reports on $Bi_2Sr_2CaCu_2O_{8+\delta}$ (Bi2212). This is due in part to the complex termination of the cleaved surfaces in YBCO, but also to the fact that most ARPES studies of YBCO have focused on $YBa_2Cu_3O_{7-\delta}$ (Y123), which has double CuO_2 planes and a single CuO chain per unit cell. Y123 has fractional oxygen stoichiometry in the chains and this leads to complications from the ordering of oxygen atoms. The resulting unstable surface makes ARPES spectra difficult to interpret [4]. Since YBCO and Bi2212 have similar superconducting properties it is important to compare the electronic properties of these two materials in order to identify which features are common and thus may be a factor in the pairing mechanism. Recently, there have been a large number of studies on the bilayer splitting in Bi2212 [6–8]. Despite this effort, it is still unclear whether bilayer splitting plays any role whatsoever in the pairing mechanism of the cuprates. We address these issues by performing ARPES measurements on $YBa_2Cu_4O_8$ (Y124), which is naturally detwinned, in contrast to Y123. Y124 has double CuO chains, one of them being translated by $b/2$ along the b axis versus the other causing a doubling of the c axis. The chains share edges and each oxygen in the chains is coordinated to three copper atoms [9] rather than two as in Y123. Y124 has a fixed oxygen stoichiometry that results in a much more stable surface and avoids problems due to oxygen ordering. Like its Y123 cousin [10], Y124 has one preferred cleavage site, which lies between the BaO plane (which is insulating and remains attached to the CuO_2 planes) and a CuO chain layer. After cleaving, two different regions: plane and chain domains are present on the sample surface. Previous studies presented spatially averaged data that was consistent with a mixture of plane and chain states. Our use of microprobe ARPES (μARPES) with a very small (50–100 μm) UV beam has permitted us to obtain spatially resolved data and thus disentangle and independently study the electronic structure of the plane and chain domains.

Twin-free single crystals of underdoped $YBa_2Cu_4O_8$ with $T_c = 80$ K were grown by the self-flux method under high oxygen pressure [11]. The ARPES experiments were carried out using a Scienta SES2002 and R4000 hemispherical analyzers mounted on the PGM beam line at the Synchrotron Radiation Center (SRC), Wisconsin, and beam line 7.0.1 of the Advanced Light Source (ALS). The energy and momentum resolution were set at ~15 meV and 0.15°–0.30° respectively for a photon energy ($h\nu$) of 28 eV. All spectra were measured at 40 K.

Figure 1(a) shows a typical ARPES intensity map at the Fermi energy for Y124 measured at $h\nu = 105$ eV over a wide area of the Brillouin zone. The 2D Fermi surface centered at S and the 1D Fermi surface along Γ-X are superimposed because the size of the chain and plane domains is smaller than the UV beam and the ARPES

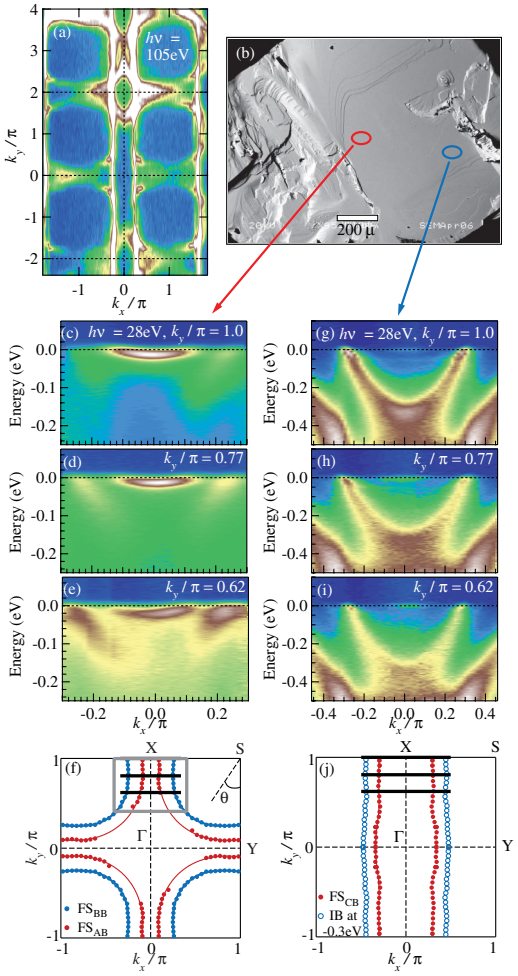

FIG. 1 (color). (a) ARPES intensity at the Fermi energy measured at $h\nu = 105$ eV. (b) SEM image of the cleaved sample surface. The blue (red) oval indicates the location of the chain (plane) domains and their size represents the approximate area of the UV beam. ARPES intensity maps at $h\nu = 28$ eV for CuO_2 planes (c),(d),(e) and CuO chains (g),(h),(i) from regions marked in (b) [data measured along the solid lines in (f) and (j)]. (f) Plane Fermi surface (FS) of the antibonding band (FS_{AB}) and bonding band (FS_{BB}). Gray rectangle marks area of collected data that was reflected about the Γ-S lines. (j) Chain FS of the conduction band (CB) and energy contour at $\varepsilon = -0.3$ eV of the insulating band (IB). Circles mark $\boldsymbol{k}_F$ obtained from MDCs. Solid lines are the tight binding fit.

signal was collected from both domains. In panel (b) we show a scanning electron microscope (SEM) picture of the sample surface after the ARPES experiment. The cleaved surface is not nearly as perfect as that typically seen in Bi2212, however, it has a number of very flat areas. By using a very small (50–100 μm) UV beam we were able to obtain ARPES data directly from these flat areas and identify two types of domains. The first displayed properties consistent with the 2D electronic structure of the CuO_2 planes, thus we will refer to it as the ''plane domain''. The location of the plane domain in Fig. 1(b) is marked by a red oval (scaled to represent the size of the UV beam). The second (marked by a blue oval) had the characteristic properties of the 1D CuO chains, thus we refer to it as the ''chain domain.''

In Figs. 1(c)–1(e), we show μARPES data measured in the plane domain along several momentum cuts. The two features seen in the data arise from bilayer splitting: a bonding band (BB) at high binding energy and an antibonding band (AB) that lies close to the Fermi energy. We determined the Fermi surfaces of BB and AB [Fig. 1(f)] by plotting the peak positions of the momentum distribution curves (MDCs) at the chemical potential. From the enclosed areas of the Fermi surfaces, we estimate the hole-carriers occupying AB and BB to be 1.44 ± 0.01 holes/Cu and 1.02 ± 0.01 holes/Cu, respectively. From the average of these numbers we determine the amount of carrier-doping (p) in the planes to be $p = 0.23 \pm 0.02$ holes/Cu. Because it is well known that samples with a p of 0.23 holes/Cu in $La_{2-x}Sr_xCuO_4$ (LSCO) are heavily overdoped, the top-most plane layer in Y124 is likely to be heavily overdoped and different from the bulk. The spectra do not show a superconducting gap down to the lowest temperature of 13 K, which supports the idea of a heavily overdoped topmost layer. The different doping of the bulk and surface layers is easily understood. Normally the chains play the role of charge reservoirs and decreasing the amount of oxygen in the chains (in the case of Y123) leads to underdoped planes. Cleaving disconnects the chain layer from the plane and breaks the bonds to the Cu atoms. As a result, the surface plane becomes overdoped.

Figures 1(g)–1(i) show the μARPES chain data. Two bands are clearly seen. The higher energy band is conducting and the lower energy one is insulating. The former has sharp quasiparticle peaks and the latter has a large energy gap of $\sim$240 meV. The 1D character of both bands is revealed in Fig. 1(j), which shows the Fermi surface of the conduction band, FS_{CB}, and an energy contour at $\varepsilon = -0.3$ eV of the insulating band.

The signal from the chain domains consists almost entirely of the 1D chain bands and similarly the plane domain signal consists almost entirely of the 2D plane bands. This indicates that the conduction electrons in Y124 are well confined within the planes and chains.

We now investigate the photon energy dependence. Figures 2(a)–2(c) show the ARPES intensity maps for the plane domains measured along a X-S cut at $h\nu = 55$, 57 and 60 eV, respectively. The corresponding energy distribution curves (EDCs) are shown in Figs. 2(d)–2(f). The BB has a higher intensity at $h\nu = 55$ eV, whereas the AB dominates the spectra at $h\nu = 60$ eV. At $h\nu = 57$ eV the intensity of both bands is equally intense. Such anticorrelation is typical for bonding and antibonding bands due to the orthogonality of their wave functions [12]. These findings, along with the result that the AB EDCs taken at 60 eV [Fig. 2(f)] show a single peak without a ''peak-dip-hump'' structure usually attributed to many-body effects [13,14], lead us to conclude that the two-peak structure observed in the EDCs is due to bilayer band splitting. In

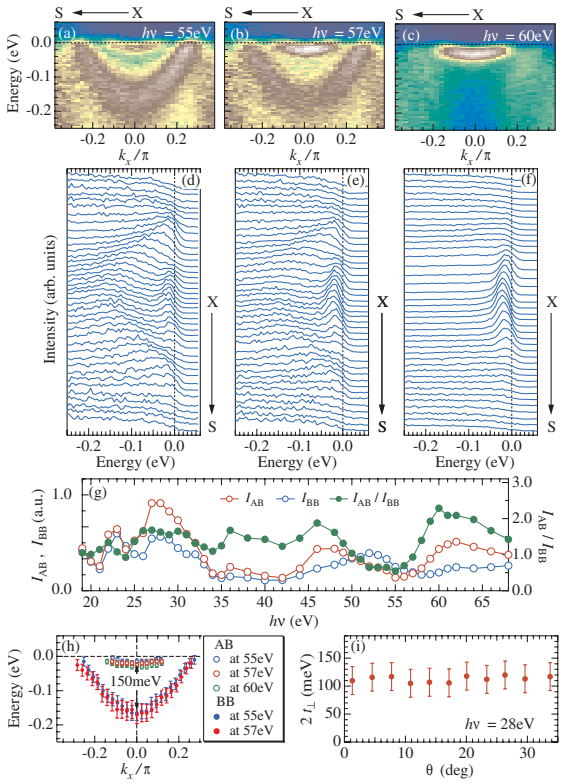

FIG. 2 (color). ARPES intensity maps for the plane domains (a),(b),(c) and corresponding EDCs (d),(e),(f) measured along the $X - S$ direction at $h\nu = 55$, 57, and 60 eV. (g) Photon energy dependence of the intensity at $\boldsymbol{k}_F$ near X in the AB (I_{AB}) and BB (I_{BB}), and their ratio. (h) Dispersion determined from the EDC peak positions in (d)–(f). Arrow represents the bilayer splitting energy ($2t_\perp$) of 150 meV at X. (i) Fermi angle θ dependence of $2t_\perp$ at $\boldsymbol{k}_F$ of AB at $h\nu = 28$ eV.

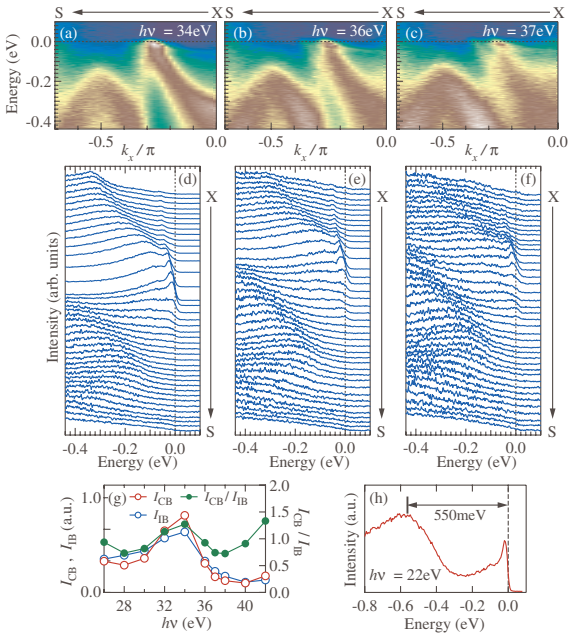

FIG. 3 (color). ARPES intensity maps of the chain domains (a),(b),(c) and corresponding EDCs (d),(e),(f) measured along $X - S$ direction at $h\nu = 34$, 36, and 37 eV. (g) Photon energy dependence of the spectral peak intensity at $\boldsymbol{k}_F$ near X for the conduction (I_{CB}) and insulating (I_{IB}) bands and their ratio, $I_{\mathrm{CB}}/I_{\mathrm{IB}}$ (see text for definition of I_{CB} and I_{IB}). (h) EDC at $\boldsymbol{k}_F$ near X of the conduction band measured at $h\nu = 22$ eV.

order to investigate the photon energy dependence of the matrix elements, we determine the spectral peak intensity of the bonding (I_{BB}) and antibonding (I_{AB}) bands by integrating the EDCs at $\boldsymbol{k}_F$ over an energy range of -70 meV $\leq \omega \leq 5$ meV. I_{BB}, I_{AB} and the ratio I_{AB}/I_{BB} measured at various photon energies are shown in Fig. 2(g). Their behavior is similar to that of the matrix elements previously reported in Bi2212 [15,16], although in the case of Y124 the overall curves are shifted to higher energy by ~6 eV. We determine the band dispersion of the bonding and antibonding bands from the peak positions of the EDCs in Figs. 2(d)–2(f). The results are shown in Fig. 2(h). Note that the energy location of each band does not significantly depend on the photon energy. Thus there is no observable k_z dispersion. While electron hopping between two CuO planes within the unit cell is significant and gives rise to large bilayer splitting, the lack of k_z dispersion indicates that hopping between unit cells is rather small. The energy of the band splitting at X ($2t_\perp$, where $t_\perp$ is the hopping integral) is estimated to be ~150 meV, which is about 4 times smaller than that (~600 meV) obtained by band calculation [17,18]. This suppression of bilayer hopping may be a result of strong electron correlations within the planes. In overdoped Bi2212, $2t_\perp$ at (π, 0) is reported to be ~100 meV, 1.5 times smaller than in Y124. The results indicate stronger c-axis coupling between double planes in Y124, and are consistent with the fact that the Y^{3+} ion is smaller than the Ca^{2+} ion separating the double planes in Y124 and Bi2212, respectively. Figure 2(i) shows $2t_\perp$ at various $\boldsymbol{k}_F$s for the antibonding band in Y124 as a function of Fermi angle θ [defined in Fig. 1(f)]. We find that $2t_\perp$ is almost constant around FS_{AB}. This is remarkably different from overdoped Bi2212, where $2t_\perp$ is nearly zero at the node. Since the superconducting properties (critical temperature, symmetry of the order parameter) of both compounds are very similar this striking difference in the properties of the bilayer splitting strongly indicates that bilayer splitting has no direct effect on the pairing mechanism. Band calculations [17,18] suggest that the nonzero $2t_\perp$ at the node is due to interlayer hopping between the Cu $3d$ (d_{zx}-d_{zx} and d_{zy}-d_{zy} π-orbitals hopping) via the Y ion. The almost constant $2t_\perp$ around FS_{AB} indicates that the interlayer hybridization between the π-orbitals via the Y ion is relatively strong compared to that between the Cu $4s$ σ-orbitals, which dominate $2t_\perp$ around (π, 0).

Figures 3(a)–3(c) show typical examples of the ARPES intensity maps along X-S for the chain domains measured at $h\nu = 34$, 36, and 37 eV, respectively. The corresponding EDCs are shown in Figs. 3(d)–3(f). The conduction band

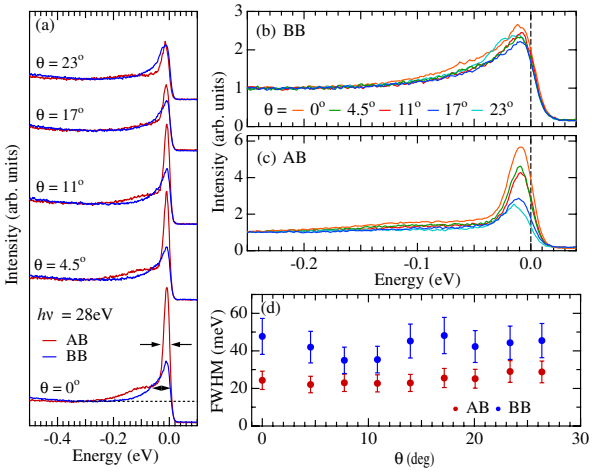

FIG. 4 (color online). (a) EDCs measured at various $\boldsymbol{k}_F$s of the BB and AB in the CuO_2 planes using 28 eV photons. All spectra are normalized to the intensity at $\varepsilon = -0.3$ eV. Superimposed EDCs at various $\boldsymbol{k}_F$s of the (b) BB and (c) AB. (d) Full width at half maximum (FWHM) of the AB and BB EDCs as a function of angle θ. Estimation method of EDC width is shown by arrows in (a).

with quasiparticle peaks around the Fermi energy and the insulating band with an energy gap of ~240 meV at $\boldsymbol{k}_F/\pi = (-0.5, 1.0)$ are observable. We should comment that a "peak-dip-hump" shape is seen in the conduction band spectra. Figure 3(h) shows the EDC measured at $\boldsymbol{k}_F$ for the conduction band. The spectral peak at $\varepsilon = -550$ meV represents the energy state of the insulating band, indicating that the conduction and insulating bands are separated by ~550 meV. We estimate the intensity of the spectral peaks in both bands, I_{CB} (I_{IB}), by integrating the EDCs over an energy range of $-190 \le \omega \le 10$ meV ($-350 \le \omega \le -150$ meV) at $\boldsymbol{k}_F$. The resulting intensities for various photon energies are shown in Fig. 3(g). This data may indicate that the conduction and insulating bands arise from bilayer splitting of the double chains. However, a band calculation [19] has estimated $2t_\perp = 36$ meV, which is much smaller than the separation energy (~550 meV) between the two observed bands. The origin of the insulating 1D band is not clear at the moment, and further theoretical effort is necessary to understand it. Details of the electronic properties of the CuO chains are discussed separately [20].

The lifetime of the quasiparticles is an important quantity for understanding the electron scattering mechanism and it can be obtained directly from the peak width of the ARPES spectra [21]. Figure 4(a) shows EDCs at various $\boldsymbol{k}_F$s for the BB and AB measured at 28 eV. All spectra are normalized to the intensity at $\varepsilon = -0.3$ eV. We first observe that the peak width in both BB and AB is almost independent of $\boldsymbol{k}_F$, while the matrix element effect produces a strong $\boldsymbol{k}_F$ dependence of the spectral intensity in AB. The almost constant peak width around the Fermi surface is even more evident from Figs. 4(b) and 4(c), where we superimpose the EDCs at $\boldsymbol{k}_F$ for the BB and AB, respectively. We estimate the peak width [see arrows in Fig. 4(a)] from the full width at half maximum (FWHM) of the EDC with the background subtracted. The peak width in the bonding band is about 1.5 times larger than in the antibonding [shown in Fig. 4(d)], indicating that electron scattering is stronger in the former. Further theoretical studies are necessary to explain this rather unexpected behavior. It may be related to the fact that the wave functions of the bonding and antibonding states are concentrated in different parts of the unit cell, but the exact mechanism has yet to be understood [22].

In conclusion, we find that the conduction electrons are well confined within the CuO_2 planes and CuO chains with a very weak hybridization. The differences in the value and momentum dependence of the bilayer splitting between Bi2212 and Y124 indicate that it is not likely to play a role in the pairing mechanism. The lifetime of the quasiparticles in the bonding band is 1.5 times shorter than in the antibonding band. The origin of this surprising difference has yet to be understood theoretically.

We thank O. K. Andersen and J. Schmalian for useful remarks. This work was supported by Basic Energy Sciences, U. S. DOE and Swiss NCCR MaNEP. The Ames Laboratory is operated for the U. S. DOE by Iowa State University under Contract No. W-7405-ENG-82. The Synchrotron Radiation Center is supported by NSF No. DMR 9212658. ALS is operated by the U. S. DOE under Contract No. DE-AC03-76SF00098. R. K. gratefully acknowledges support of K. Alex Müller Foundation.

[1] J. C. Campuzano *et al.*, Phys. Rev. Lett. **64**, 2308 (1990).
[2] K. Gofron *et al.*, Phys. Rev. Lett. **73**, 3302 (1994).
[3] M. C. Schabel *et al.*, Phys. Rev. B **57**, 6090 (1998).
[4] D. H. Lu *et al.*, Phys. Rev. Lett. **86**, 4370 (2001).
[5] S. V. Borisenko *et al.*, Phys. Rev. Lett. **96**, 117004 (2006).
[6] S. V. Borisenko *et al.*, Phys. Rev. Lett. **96**, 067001 (2006).
[7] A. A. Kordyuk *et al.*, Phys. Rev. B **70**, 214525 (2004).
[8] S. V. Borisenko *et al.*, Phys. Rev. B **69**, 224509 (2004).
[9] P. Fischer *et al.*, Solid State Commun. **69**, 531 (1989).
[10] D. J. Derro *et al.*, Phys. Rev. Lett. **88**, 097002 (2002).
[11] J. Karpinski *et al.*, Nature (London) **336**, 660 (1988).
[12] A. Bansil *et al.*, Phys. Rev. Lett. **83**, 5154 (1999).
[13] Z.-X. Shen *et al.*, Phys. Rev. Lett. **78**, 1771 (1997).
[14] A. Kaminski *et al.*, Phys. Rev. Lett. **86**, 1070 (2001).
[15] J. Mesot *et al.*, Phys. Rev. B **63**, 224516 (2001).
[16] A. A. Kordyuk *et al.*, Phys. Rev. Lett. **89**, 077003 (2002).
[17] O. K. Andersen *et al.*, J. Phys. Chem. Solids **56**, 1573 (1995).
[18] O. K. Andersen *et al.*, Phys. Rev. B **49**, 4145 (1994).
[19] T. F. A. Müller *et al.*, Phys. Rev. B **60**, 1611 (1999).
[20] R. Khasanov *et al.*, cond-mat/0609385.
[21] A. Kaminski *et al.*, Phys. Rev. Lett. **84**, 1788 (2000).
[22] E. Pavariani *et al.*, Phys. Rev. Lett. **87**, 047003 (2001).